Int J Adv Manuf Technol (2009) 41:1051–1058
DOI 10.1007/s00170-008-1557-7

ORIGINAL ARTICLE

Temperature distribution in the workpiece due to plane magnetic abrasive finishing using FEM

Gurvinder Kumar · Vinod Yadav

Received: 3 November 2007 / Accepted: 2 May 2008 / Published online: 17 June 2008

Abstract A mathematical model is developed for the prediction of magnetic potential using Maxwell's equations and finite element method is used to find the magnetic potential distribution within the gap between tool bottom surface and workpiece top surface. From magnetic potential model, the magnetic pressure developed and corresponding heat flux generated on workpiece surface are evaluated. Further a mathematical model is developed for heat transfer in the workpiece and again finite element method is used for the prediction of temperature rise in the workpiece. The effects of various operating input parameter on magnetic potential distribution in the gap and temperature rise in the workpiece has been studied.

Keywords MAF · Magnetic abrasive particle · Magnetic potential · Temperature · FEM

Nomenclature

A	Abrasive particle (μm)
D	Mean diameter of the magnetic particle (μm)
d	Mean diameter of the abrasive grain (μm)
B	Magnetic flux density *(tesla)*
E	Electric field intensity *(V/m)*
f	Friction
J	Electric current density *(A/m^2)*
H	Magnetic field strength in the working zone *(A/m)*
H_a	Magnetic field strength in the air-gap *(A/m)*
μ_o	Magnetic permeability in vacuum *(N/A^2)*
μ_r	Relative permeability of pure iron
μ	Permeability of pure iron *(H/m)*
ε	Permittivity *(farad/m)*
ρ	Charge density
χ_m	Magnetic susceptibility
M	Magnetization
ϕ	Magnetic potential (AT)
l_b	Length of brush from workpiece to electromagnet
r_0	Radius of electromagnet
P	Magnetic pressure supplied by the magnet (Pa)
w	Volume ratio of iron in a magnetic particle
T	Temperature (°C)
q_w	Heat flux going inside the workpiece (W/m^2)
q_t	Total heat flux (W/m^2)
K_w	Thermal conductivity of workpiece (W/mK)
K_a	Thermal conductivity of magnetic abrasive particle (W/mK)
μ_f	Coefficient of workpiece
v	Velocity of abrasive particles (m/s)
R_w	Energy partition
β_w	Geometric mean thermal property of workpiece
β_a	Geometric mean thermal property of abrasive particle
ρ_w	Density of workpiece (Kg/m^3)
ρ_a	Density of magnetic abrasive particle(Kg/m^3)
C_w	Specific heat of workpiece (J/Kg-K)
C_a	Specific heat of magnetic abrasive particle (J/Kg-K)
D_0	Diameter of electromagnet (m)
N	rpm of magnetic abrasive particles

Superscript

e	Element
T	Transpose

Subscript

D	Domain

G. Kumar
Energy Technologies Department, NTPC LTD.,
Noida, India
e-mail: gurvinderkumar@ntpc.co.in

V. Yadav (✉)
Mechanical Engineering Department,
Motilal Nehru National Institute of Technology,
Allahabad, India
e-mail: vinody@mnnit.ac.in

B Boundary
w Workpiece

1 Introduction

Magnetic abrasive finishing (MAF) is an ultra-precision finishing process in which an electromagnetically generated magnetic energy is used for finishing purpose. The process involves finishing action through a tool called a magnetic abrasive brush formed in magnetic field from magnetic abrasive particles composed of ferromagnetic material (such as iron particles) and abrasive grains (like $A1_2O_3$, SiC, Cr_2O_3, or diamond). There are basically two types of magnetic abrasive particles, namely bonded and unbonded, used in the MAF process.

In bonded type, we take the powder of both iron and abrasive, blending the two properly and then sintering, followed by crushing, giving the magnetic abrasive particles. The enlarged view of a magnetic abrasive particle is shown in Fig. 1, with base as iron and the abrasive grains are attached to it [1]. It is assumed to be spherical in shape of diameter D with nominal diameter of abrasive grains as d. Generally the value of D ranges from 100 to 400 μm whereas value of d lies between 1 to 30 μm, according to the use and requirement. In bonded type, the base iron causes the motion of the magnetic abrasive particle in the magnetic field and the abrasive grains are responsible for the finishing. In unbonded type, we make the mixture of iron powder and abrasive powder and blending it so that the mixture becomes almost homogeneous. In this case when the particle of iron moves due to magnetic field, it collides with the abrasive grains and provides the motion so that the abrasive action takes place.

The setup of MAF process consists of two magnetic poles *S* and *N* and the workpiece is placed between the two poles Fig. 2. The gap between the magnetic poles and the workpiece is filled with the magnetic abrasive particles. When the power is applied to the poles, magnetic field generates the necessary finishing pressure between the poles and the magnetic abrasive particles are joined to each other

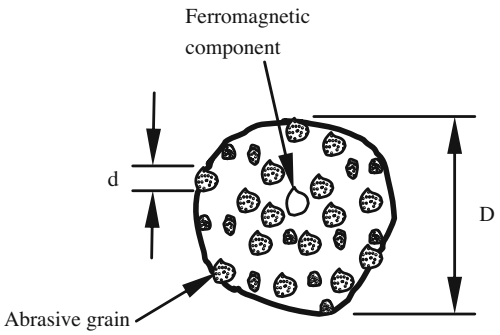

Fig. 1 Enlarged view of magnetic abrasive particle

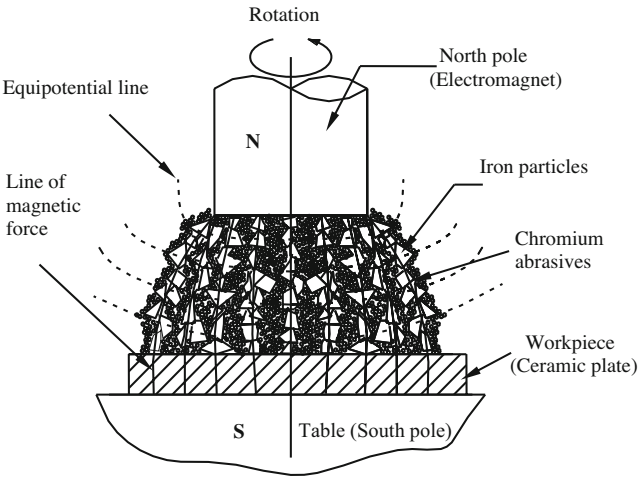

Fig. 2 Schematic diagram of MAF showing finishing using (Cr_2O_3-Fe) magnetic particles

magnetically between the magnetic poles *S* and *N* along the lines of magnetic force, forming a flexible magnetic abrasive brush. Consider the magnetic abrasive particle '*A*' as shown in Fig. 3 on which two forces F_Z (along the lines of magnetic force) and F_R (along the equipotential magnetic line) act simultaneously, and F shows their resultant. The magnetic force F_R is responsible for actuating the abrasive particles such that they take part in finishing the workpiece. The force F_Z acts on the abrasive grains in the magnetic particle is mainly responsible for the cutting action. Any change in the strength of the magnetic field (H) in the direction of the line of magnetic force near the workpiece surface will actuate the magnetic abrasive particles. The effective way of changing the force and the rigidity of the magnetic abrasive brush is through the change in D. Hence, ferromagnetic particles of several times the diameter of the magnetic abrasives (d) are mixed to form the magnetic abrasive brush.

In the case of plane workpiece, we make rotating north pole. If the workpiece is of ferrous material, we make south pole of workpiece itself. Hence a magnetic force and pressure exist between the north and the south poles. Thus magnetic abrasive particles remain bonded within the working domain. But if the workpiece is of some different material as shown in Fig. 2 [2], then we put a south pole

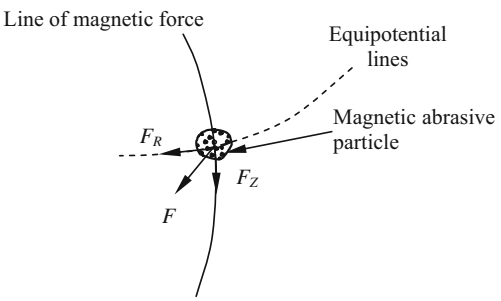

Fig. 3 Enlarged view of forces acting on magnetic abrasive particle *A*

below the non-ferrous workpiece so that force still exists between the north pole and the south pole for generating magnetic pressure. To finish the whole surface of workpiece, the table reciprocates both in x and y axes whereas the rotating north pole rotates at one point.

2 Mathematical modeling

The modeling of machining process can be defined from the manufacturing engineer's point of view as a simplified mathematical formulation of a machining process which establishes a relation between input and output quantities in order to describe the dynamic as well as the static performance of the machining process. The purpose of modeling a machining operation is to develop predictive capability for machining performance well in advance and finally to achieve optimum productivity, quality, and cost. The mathematical model of a machining operation is required mainly for simulation of process, for design and optimization of process and also to Control a process. MAF is mainly developed for higher accuracy, but high temperature affects the performance of workpiece to be finished, so temperature model during MAF process has been developed. But as temperature is a function of magnetic potential (ϕ), so magnetic potential model is also required.

2.1 Assumptions

(i) The domain is considered to be axisymmetric for the magnetic brush and workpiece due to the symmetrical nature around the central axis.
(ii) The workpiece material is homogeneous and isotropic.
(iii) The eddy current and core losses generated during the process are neglected.
(iv) Magnetic abrasive particles are identical and spherical in shape, and they follow a particular circular track continuously.
(v) The magnetic brush rotates at the same rpm as the tool.
(vi) There is no fluctuation in current during the process and magnetic field is uniformly saturated in the magnetic brush.
(vii) Thermal properties like thermal conductivity, specific heat, and density of work-material are temperature independent.
(viii) The variation of temperature and magnetic potential is assumed to be time independent (steady state condition).

2.2 Magnetic potential model

In electromagnetic field problems, governing laws can be expressed concisely by a single set of four equations. These equations are known as Maxwell's equations [6] and are as written below:

$$\left.\begin{array}{ll} \nabla \times E = 0, & \nabla \times H = J \\ \nabla \cdot E = \frac{\rho}{\varepsilon}, & \nabla \cdot H = 0 \end{array}\right\} \quad (1)$$

In the working zone, J=0 because there is no electric current. The magnetic potential is related to H and relationship can be written as [6]

$$H = -\nabla\phi \quad (2)$$

Using equations (1) and (2), we can write

$$\nabla^2\phi = 0 \quad (3)$$

The steady state Laplacian form of this equation within axisymmetric domain can be written as

$$\frac{1}{r}\frac{\partial}{\partial r}\left(r\frac{\partial\phi}{\partial r}\right) + \frac{\partial^2\phi}{\partial z^2} = 0 \quad (4)$$

As magnetic potential is responsible for the shape and size of brush after applying the magnetic field, hence shape and size of magnetic brush is considered as the domain for finding the magnetic potential. The domain along with the boundary conditions is shown in Fig. 4. The value of ϕ_1 at boundary can be calculated using the following equation [6]:

$$\phi_1 = \frac{Bl_b}{\mu_0(1+\chi_m)} \quad (5)$$

The radius of magnetic brush can be calculated using the equation.

$$r^2 = -2r_0\left[z - \left(\frac{r_0}{2} + l_b\right)\right] \quad (6)$$

The velocity of magnetic abrasive particles depends upon the rpm of tool (N pole of electromagnet) and the track followed by the magnetic abrasive particles. Here we are assuming that the particular magnetic abrasive particles are

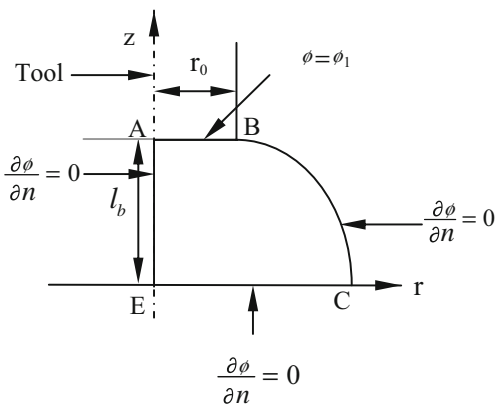

Fig. 4 Domain showing boundary condition for magnetic potential model

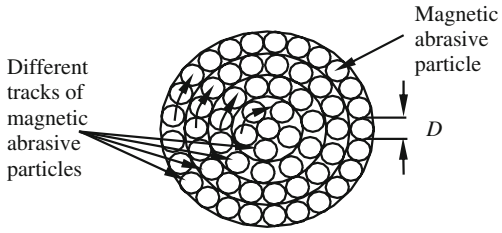

Fig. 5 Schematic diagram of different tracks followed by magnetic abrasive particles

continuously following a particular path as shown in Fig. 5. The velocity of magnetic abrasive particle in the track 1 can be calculated using Eq. (7).

$$\left.\begin{array}{l} v = \frac{\pi \times D \times N}{60}\,(m/s) \\ \text{where } D = \text{mean diameter of magnetic abrasive particle} \\ \quad\quad N = \text{rpm of magnetic abrasive particle} \end{array}\right\} \tag{7}$$

Similarly for track 2, 3, and so on tracks, the velocity will become $2v$, $3v$ and so on, respectively.

The magnetic pressure between the abrasive and the workpiece can be written as [3]:

$$P = \mu_0 \frac{H_a^2}{4} \frac{3\pi(\mu_r - 1)w}{3(2+\mu_r) + \pi(\mu_r - 1)w} \quad \text{where} \quad H_a = \frac{\mu_r + 2}{3} H \tag{8}$$

2.3 Temperature model

During finishing of workpiece, there is generation of heat flux at the surface of workpiece due to machining pressure and friction between workpiece and abrasives. The rate of heat generation at the surface of workpiece for few seconds is so high that there is very high temperature rise, which will be responsible for generation of residual stresses inside the workpiece. The governing equation for steady state temperature distribution in an axisymmetric workpiece domain can be written as follows:

$$K_w \left\{ \frac{1}{r}\frac{\partial}{\partial r}\left(r\frac{\partial T}{\partial r}\right) + \frac{\partial}{\partial z}\left(\frac{\partial T}{\partial z}\right) \right\} = 0 \tag{9}$$

The domain for temperature model along with the boundary conditions is shown in Fig. 6.

2.4 Calculation of heat flux

The pressure generated between the abrasives and workpiece and coefficient of friction are responsible for generation of heat flux. The high velocity abrasives are rubbing the workpiece top surface and due to friction and high magnetic pressure, heat flux is generated. The total heat flux generated because of abrasives can be calculated as follows:

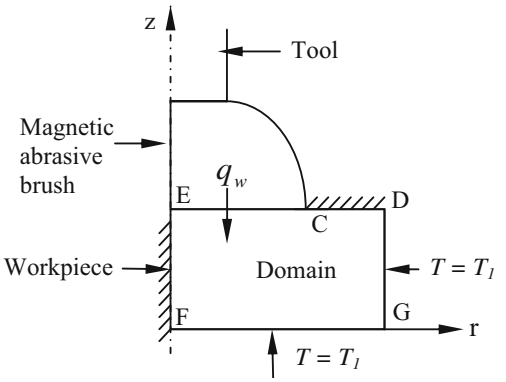

Fig. 6 Domain showing boundary condition for temperature model

$$q_t = P \times \mu_f \times v \tag{10}$$

The heat flux entering to workpiece can be written as:

$$q_w = R_w \times P \times \mu_f \times v \tag{11}$$

Here R_w is energy partition and calculated as $R_w = \frac{\beta_w}{\beta_w + \beta_a}$ where $\beta_w = \sqrt{K_w \rho_w C_w}$ and $\beta_a = \sqrt{K_a \rho_a C_a}$ [7]

3 Finite element formulations

3.1 Magnetic potential model

The *Galerkin's FEM* is one among the class of techniques collectively known as the method of weighted residue [5]. In *Galerkin's* method, we select the weight functions and set the weighted average of residue to zero or in mathematical terms, we can say the residue is made orthogonal to the weight functions. By applying Galerkin's approach to Eq. (4), the elemental equations over a typical element is given by

$$[K_1]^e \{\phi\}^e = 0 \tag{12}$$

Here, $[K_1]^e$ is the elemental coefficient matrix and $\{\phi\}^e$ is the magnetic scalar potential vector of the respective element. The elemental coefficient matrix is evaluated by $[K_1]^e = \int_{D^e} [B]^{eT}[B]^e r dr dz$ where, $[B]^e$ is derivative of shape function matrix, D^e is the domain of the area element. In the present case eight-noded isoparametric elements are chosen for the finite element approximation. The integrals in Eq. 12 for eight-noded isoparametric quadrilateral element are computed numerically using Gaussian quadrature with three points in each direction. All the elemental equations are assembled to get a global set of algebraic equation, which is represented as

$$[GK_1]\{\phi\} = 0 \tag{13}$$

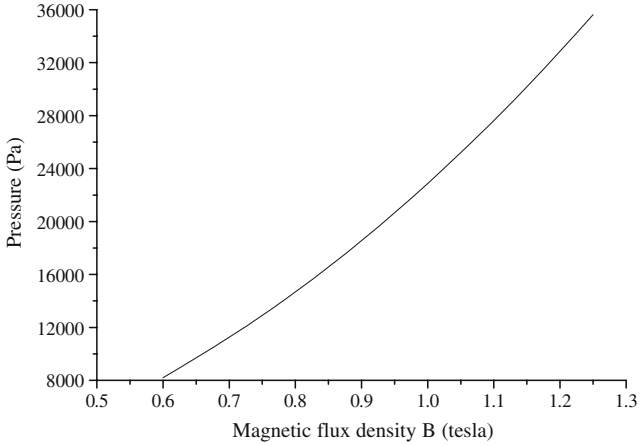

Fig. 7 Variation of machining pressure with different magnetic flux density

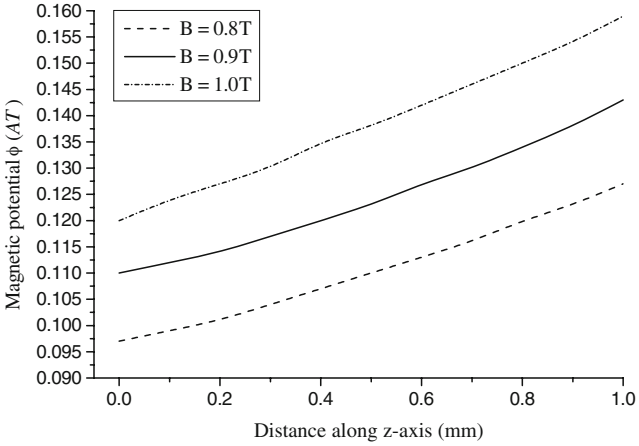

Fig. 9 Variation of f along z-axis at r=0 at 5835 rpm of tool. Other machining condition are given in Table 1

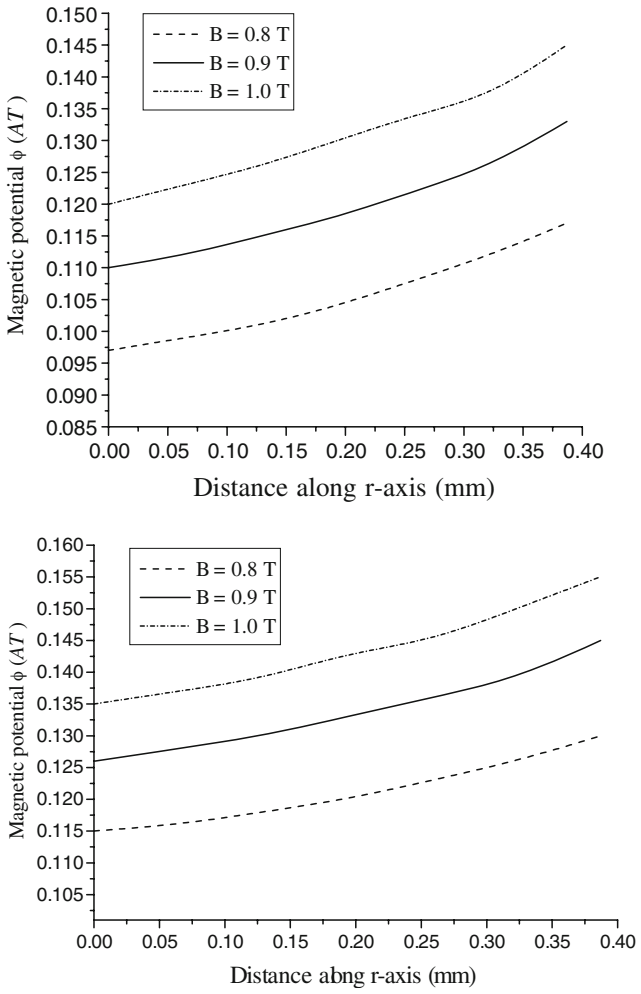

Fig. 8 Variation of f along radius at bottom of magnetic brush at (a) z=0 (b) z=0.5 mm at 5835 rpm of tool. Other machining condition are given in Table 1

where $[GK_1]$ is the global coefficient matrix and $\{\phi\}$ is the global magnetic scalar potential vector. Essential boundary conditions are applied in Eq. 13 and finally solved by Gauss elimination method to find nodal magnetic scalar potential.

Table 1 Machining conditions [2, 4]

Machining parameters	Description
Material of workpiece	Silicon nitride (Si_3N_4)
Magnetic abrasive powder	*Chromium oxide* (Cr_2O_3)
Radius of the workpiece	10 *mm*
Thickness of workpiece	2.5 *mm*
Working gap	1 *mm*
Tool (electromagnet) diameter	6 *mm*
Volume ratio of the iron in magnetic abrasives	0.5
Mean diameter of the magnetic particles	387 μm
Magnetic grain (Cr_2O_3) diameter	3 μm
RPM of tool	5835
Value of energy partition	*0.41*
Coefficient of friction	*0.6*
Permeability of free space	$\mu_0 = 4\pi X10^{-7}$ *H/m*
Relative permeability of pure iron	$\mu_r = 5000$ [8]
Thermal conductivity of silicon nitride (Si_3N_4)	29.3 *W/mK*
Thermal conductivity of chromium oxide (Cr_2O_3)	31.8 *W/mK*
Thermal conductivity of iron (*Fe*)	73.3 *W/mK*
Specific heat of silicon nitride (Si_3N_4)	650 *J/KgK*
Specific heat of chromium oxide (Cr_2O_3)	250 *J/KgK*
Specific heat of iron (*Fe*)	444 *J/KgK*
Density of silicon nitride (Si_3N_4)	3243 Kg/m^3
Density of chromium oxide (Cr_2O_3)	5200 Kg/m^3
Density of iron (*Fe*)	7870 Kg/m^3

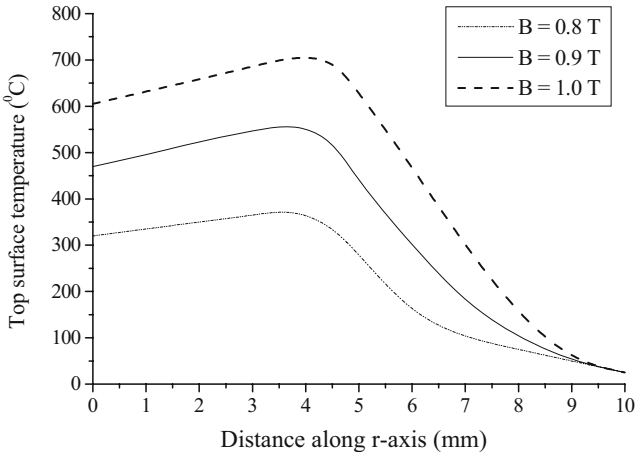

Fig. 10 Variation of temperature along radius at top surface of workpiece for 5835 rpm of tool. Other machining condition are given in Table 1

3.2 Temperature model

By applying Galerkin's approach to Eq. (9), the elemental equations over a typical element is given by

$$[K_2]^e\{T\}^e = \{f\}^e \tag{14}$$

where the elemental coefficient matrix $[K_2]^e$ can be written as

$$[K_2]^e = K_w \int_{D^e} [B]^{eT}[B]^e r dr dz \tag{15}$$

and right-side force vector can be written as

$$\{f\}^e = \int_B \{N\}^b q_w r dB \tag{16}$$

All the elemental equations for temperature are assembled to get a global set of algebraic equation, which is written as,

$$[GK_2]\{T\} = \{GF\} \tag{17}$$

where $[GK_2]$ is the global coefficient matrix, $\{GF\}$ is the global right-side force vector, and $\{T\}$ is the global temperature rise vector. Essential boundary conditions are applied in Eq. 17 and finally solved by Gauss elimination method to find temperature rise.

4 Results and discussion

In the present work, SIMU-MAF software has been developed using MATLAB, which is validated by comparing the results of a known problem from the literature, for the simulation of magnetic potential and temperature. For the use of this developed software IDEAS is used as a preprocessor.

Figure 7 shows that as the magnetic flux density increases, the machining pressure also increases. With increase in magnetic flux density, magnetic potential increases accordingly as we move away from the centre of magnetic brush towards the end in *r*-direction. The variation of magnetic potential at the contact surface of workpiece and magnetic particles for different magnetic flux density along *r*-axis is shown in Fig. 8. The magnetic potential increases as we go away from the centre of magnetic brush, because it follows the equipotential line path. As we go near the electromagnet, the magnetic potential continuously increases, that is why more magnetic potential value is there in Fig. 8b as compared to Fig. 8a. Figure 9 shows variation of magnetic potential along *z*-axis at center of magnetic brush for various values of magnetic flux density.

When finishing ceramics workpiece (Si_3N_4) using MAF, the temperature rise in the workpiece is very high. The reason for the temperature rise in the workpiece in the case of ceramics is due to the fact that it is difficult to machine. So to finish the ceramics, a high magnetic flux density and high rpm of electromagnet are required, which results in high machining pressure and friction between magnetic particles (Cr_2O_3+ Fe) and workpiece surface.

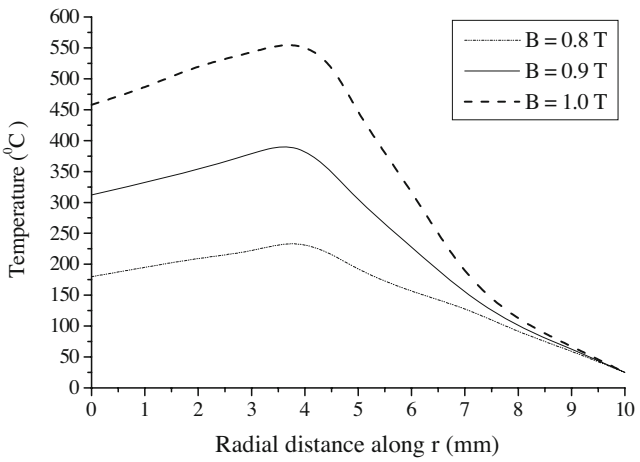

Fig. 11 Variation of temperature along radius at z=1.25 mm from bottom of workpiece at 5835 rpm of tool. Other machining condition are given in Table 1

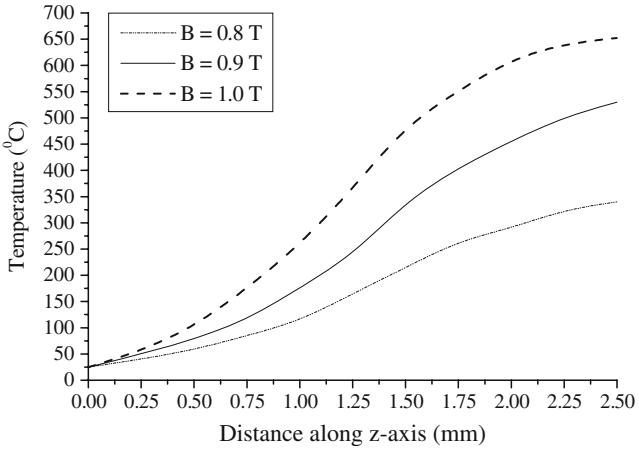

Fig. 12 Variation of temperature along *z*-axis at r=3 mm in radial direction at 5835 rpm of tool. Other machining conditions are given in Table 1

As we move away from the centre of the workpiece, the temperature increases gradually and at the end point of magnetic brush, temperature starts decreasing sharply. Figure 10 and 11 show the temperature rise at the contact surface of workpiece and magnetic particles for different magnetic flux density along r-axis at a particular rpm (5835). The maximum temperature rises upto 708°C for one tesla magnetic flux density. The reason for increase in temperature while moving away from the centre of workpiece is due to increase in magnetic particles velocity and magnetic potential. But after the end point of magnetic brush, there is no surface contact between particles and workpiece so temperature decreases sharply.

Figure 12 shows temperature rise along *z*-axis at 3 mm away from the centre of workpiece surface for different magnetic flux density. The temperature rises as we are going closer to the contact surface of workpiece and magnetic brush. Figure 13 shows temperature rise along *z*-axis at the centre of workpiece surface for different

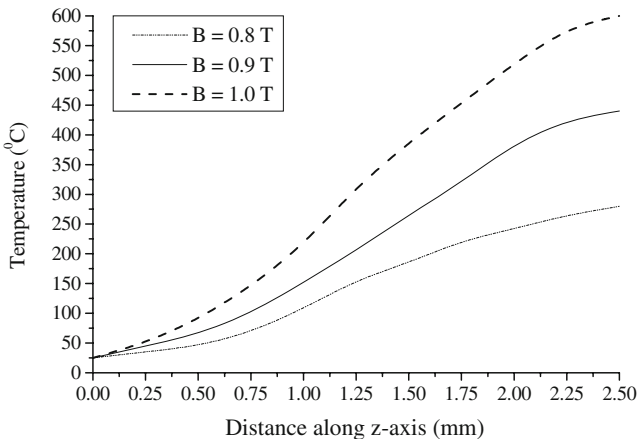

Fig. 13 Variation of temperature along *z*-axis at r=0 mm in radial direction at 5835 rpm of tool. Other machining conditions are given in Table 1

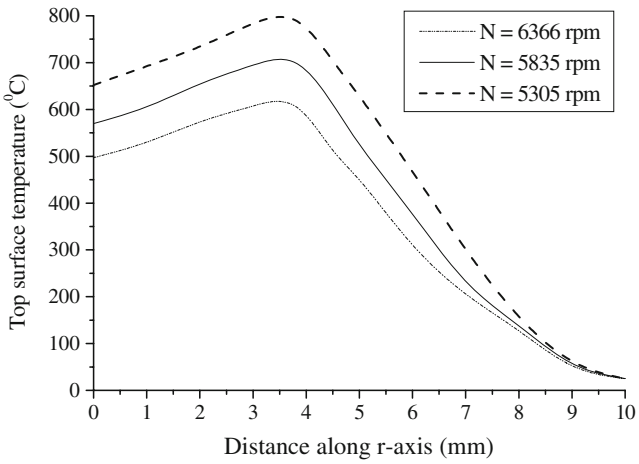

Fig. 14 Variation of temperature along radius at top surface of workpiece for different tool rpm & B=1 tesla. Other machining condition are given in Table 1

magnetic flux density. The temperature rise is more in case of r=3 mm as compare to r=0 mm due to increase in magnetic particles velocity in former case.

Figure 14 shows temperature rise along *r*-axis at the contact surface of workpiece and magnetic particles from the centre of workpiece for different *rpm* of magnetic particles at one *tesla* magnetic flux density. The maximum temperature rises from 633°*C* to 841°*C* when rpm of magnetic particles are increased from 5305 to 6366 rpm along *r*-axis. The reason for temperature rise is, as we are increasing the rpm, heat flux generated at the contact surface also increases so naturally temperature at the contact surface increases.

5 Conclusions

Various operating parameters such as magnetic flux density, magnetic pressure, magnetic potential and tool rpm have been studied and following conclusions are derived from the present analysis.

- The mathematical modeling and finite element formulation of MAF presented in this paper appear to describe the actual phenomena reasonably accurately.
- The machining pressure between the magnetic brush and the workpiece increases considerably with the increases in magnetic flux density, which further affects magnetic potential and, hence, the temperature rise in the workpiece.
- The magnetic potential increases along the radius as well as along the *z*-axis rapidly with increase in magnetic flux density.
- Temperature rise inside the workpiece along the radius firstly increases slowly upto the vicinity of *magnetic brush*, but after that it decreases sharply.

- Temperature rise increases along *z*-direction from bottom of workpiece towards top surface of workpiece.
- Temperature rise inside the workpiece is found to be increases with the increase in rpm of magnetic abrasive brush. More the rpm of magnetic abrasive brush more will be the temperature rise.
- From the results, it can be said that, firstly magnetic flux density value should be selected and then tool rpm in order to obtain smooth finished surface, with less rise in temperature inside the workpiece.

References

1. Shinmura T, Takazava K, Hitano E, Aizawa T (1987) Study on magnetic abrasive process-Effect of various types of magnetic abrasives on finishing characteristics. Journal of the Japan Society of Precision Engineering 21(2):139–141
2. Shinamura T, Wang FH (1994) A new process for precision finishing of silicon nitride fine ceramics by the application of magnetic abrasive machining using chromium-oxide abrasives mixed with iron particles. Journal of the Japan Society of Precision Engineering 28(3):229–230
3. Kim JD, Choi MS (1995) Simulation for the prediction of surface-accuracy in magnetic abrasive machining. J Mater Process Tech 53:630–642 DOI 10.1016/0924–0136(94)01753-N
4. Hou Z, Komanduri R (1998) Magnetic field assisted finishing of ceramics-part II: On the thermal aspects of magnetic float polishing (MFP) of ceramics balls. Journal of Tribology Transactions of ASME 120:652–659 DOI 10.1115/1.2833762
5. Reddy JN (2003) An introduction to finite element method, 2nd edn. Tata McGraw-Hill, New Delhi
6. Griffith DJ (2000) Introduction to electromagnetism, 3rd edn. Prentice Hall of India Pvt. Ltd, New Delhi
7. Shaw MC (1996) Principles of abrasive processing. Clarenden, Oxford
8. Seth SP (2001) A course in electrical engineering materials (Physics, Properties and Application), 2nd edn. Dhanapat Rai and Sons, New Delhi